Performance Improvement of GaN-Based Flip-Chip White Light-Emitting Diodes with Diffused Nanorod Reflector and with ZnO Nanorod Antireflection Layer

Hsin-Ying Lee, Yu-Chang Lin, Yu-Ting Su, Chia-Hsin Chao, Véronique Bardinal

Performance improvement of GaN-based flip-chip white light-emitting diodes with diffused nanorod reflector and with ZnO nanorod antireflection layer

Hsin-Ying Lee[1*], Yu-Chang Lin[1], Yu-Ting Su[1], Chia-Hsin Chao[2], and Véronique Bardinal[3,4]

[1]Department of Photonics, Advanced Optoelectronic Technology Center, National Cheng Kung University, Tainan 701, Taiwan, Republic of China
[2]Electronics and Optoelectronics Research Laboratories, Industrial Technology Research Institute, Hsinchu 300, Taiwan, Republic of China
[3]CNRS; LAAS; 7 avenue du colonel Roche, F-31077 Toulouse, France
[4]University of Toulouse; UPS, INSA, INP, ISAE ;LAAS; F-31077 Toulouse, France

Corresponding Author: Prof. Hsin-Ying Lee
Address: Department of Photonics, National Cheng Kung University,
Tainan 701, Taiwan
Tel: 886-6-2082368
Fax: 886-6-2082368
E-mail: hylee@ee.ncku.edu.tw

Abstract

The GaN-based flip-chip white light-emitting diodes (FCWLEDs) with diffused ZnO nanorod reflector and with ZnO nanorod antireflection layer were fabricated. The ZnO nanorod array grown using an aqueous solution method was combined with Al metal to form the diffused ZnO nanorod reflector. It could avoid the blue light emitted out from the Mg-doped GaN layer of the FCWLEDs, which caused more blue light emitted out from the sapphire substrate to pump the phosphor. Moreover, the ZnO nanorod array was utilized as the antireflection layer of the FCWLEDs to reduce the total reflection loss. The light output power and the phosphor conversion efficiency of the FCWLEDs with diffused nanorod reflector and 250-nm-long ZnO nanorod antireflection layer were improved from 23.90 mW to 21.15 mW and 77.6% to 80.1% in comparison with the FCWLEDs with diffused nanorod reflector and without ZnO anaorod antireflection layer, respectively.

Keyword: Aqueous solution method, flip-chip white light-emitting diodes, diffused nanorod reflector, ZnO nanorod

1. Introduction

Recently, people have put more and more attentions on the problems of energy shortage and environment problems. Many research teams actively investigated how to improve energy saving and how to product renewable energy. The white light-emitting diodes (WLEDs) are expected to be the promising green lighting sources and have been widely used in solid-state lighting and taken as the next generation lighting sources to replace the compact fluorescent lamp (CFL) and incandescent light. The WLEDs exhibit many superior advantages such as the long lifetime, high luminous intensity, energy saving, fast response, low heat dissipation and high reliability. In general, there are three approaches can be used to fabricate WLEDs: (1) using the blue light-emitting diodes (LEDs) to excite the yellow phosphor [1,2], (2) using an ultraviolet (UV) LEDs to excite red, green, and blue phosphors [3,4], and (3) mixing three primary colors of red, green, and blue LEDs [5]. The commercial WLEDs were commonly integrated by the GaN-based blue LEDs with yellow phosphor ($Y_3Al_5O_{12}:Ce_3^+$ or $YAG:Ce_3^+$) layer. To augment the application of WLEDs, the development of high performance WLEDs are immediately needed. Since the properties of the GaN-based blue LEDs seriously affect the performances of WLEDs, how to improve the internal quantum efficiency and external quantum efficiency of the blue LEDs are the primarily issues. In view of

the significant progress of GaN-based epitaxial technology, the internal quantum efficiency of the GaN-based blue LEDs achieved the theoretical limit of 90%. However, the large difference of refractive index between the GaN-based semiconductor (n_{GaN}=2.4) and the air (n_{air}=1) led to the increase of total internal reflection and the Fresnel loss. Generally, several methods, such as die shape [6,7], surface roughness [8,9], photonic crystal [10,11], reflector [12,13], and antireflection coating layer [14], have been reported previously to overcome the undesired total internal reflection and Fresnel loss. Among these methods, the reflector exhibits several advantages including simple fabrication, low cost, and outstanding light extraction improvement of LEDs. In this work, to improve the light extraction efficiency of WLEDs, the designed diffused nanorod reflector constructed with the 700-nm-thick Al metal and ZnO nanorod array with optimal rod-length of 500 nm was used in the flip-chip white light-emitting diodes (FCWLEDs). The detail investigation of diffused nanorod reflector was shown in previous published paper [15]. The diffused nanorod reflector could effectively increase the reflection angle and enhance the light escaping probability from the semiconductor compared with the traditional flat reflector. Furthermore, to further improve the light extraction from the light-emitted side of the FCWLEDs, the ZnO nanorod arrays were also used as the antireflection layer. Finally, the yellow phosphor layer was coated on the ZnO

nanorod antireflection layer by using the remote phosphor coating technique which possessed the uniformity and high color converted efficiency.

2. Experiment Procedure

Figure 1 shows the schematic configuration of the GaN-based FCWLEDs with diffused nanorod reflector and with ZnO nanorod antireflection layer. A metal organic chemical vapor deposition (MOCVD) system was used to grow the epitaxial layers of the GaN-based blue LEDs. A 2.8-μm-thick GaN buffer layer, a 4-μm-thick Si-doped GaN layer ($n=3\times10^{17}$ cm^{-3}), an undoped InGaN/GaN multiple quantum well (MQW) active layer, a 33-nm-thick Mg-doped $Al_{0.2}Ga_{0.8}N$ layer ($p=1\times10^{17}$ cm^{-3}), and a 150-nm-thick Mg-doped GaN layer ($p=3\times10^{17}$ cm^{-3}) were sequentially grown on the c-plane sapphire substrates. The InGaN/GaN MQW active layer was consisted of twelve pairs of 3-nm-thick $In_{0.2}Ga_{0.8}N$ well layer and 12.7-nm-thick GaN barrier layer. The fabrication processes of the conventional GaN-based LEDs are as follows. The epitaxial layer with mesa (300×300 μm^2) pattern protected by a 300-nm-thick Ni metal mask was etched down to the Si-doped GaN layer by a reactive ion etching (RIE) system. After the mesa etching, the remaining Ni metal mask was removed using aqua regia. The n-electrode Ti/Al/Ti/Au (25/100/50/150 nm) was deposited using an electron-beam evaporator. Moreover, the n-electron was treated by a rapid

thermal annealing (RTA) system with 850 ^{o}C for 2 min in a pure N_2 ambient for obtaining the good ohmic contact performance [16]. Thin Ni/Au (2.5/2.5 nm) and thick Ni/Au (20/100 nm) metal contacts were deposited on Mg-doped GaN layer as the current spreading layer (CSL) and the p-electrode, respectively. Prior to thin Ni/Au metal deposition, a surface sulfurization treatment was performed to improve the contact performance between the thin Ni/Au metals and the Mg-doped GaN mesa region [17]. The p-type ohmic contact formation was carried out in an air ambient at 500 °C for 10 min by a RTA system. When the conventional GaN-based LEDs were fabricated, and then the diffused nanorod reflector was sequentially fabricated. A 50-nm-thick Al-doped ZnO (AZO) seed layer was deposited on the Ni/Au current spreading layer using a magnetron radio frequency sputtering system. A 500-nm-long ZnO nanorod array was grown on the AZO seed layer using an aqueous solution method at 90 ^{o}C. The chemical solution was mixed by 0.025 M zinc nitrate hexahydrate ($Zn(NO_3)_2$-$6H_2O$) and 0.025 M hexamethylenetetramine ($C_6H_{12}N_4$). A 700-nm-thick Al metal was then deposited on the top of the ZnO nanorod array using an electron-beam evaporator. The morphology of diffused nanorod reflector was carried out using scanning electron microscope (SEM) and is shown in the inset of Figure 1. Then a 50-nm-thick AZO seed layer and ZnO nanorod arrays were sequentially deposited on the sapphire surface of the GaN-based FCLEDs with diffuse

nanorod reflector. To find the optimal rod-length of the ZnO nanorod in the array as the antireflection layer, the ZnO nanorods with various rod-lengths of 0, 100, 250, 500 and 700 nm were grown. Finally, the remote phosphor coating technique was used to form the GaN-based FCWLEDs. A silicone layer was spread on the 250-nm-rod-long ZnO nanorod antireflection layer and a yellow phosphor layer was covered on the silicone layer to complete the fabrication process of the FCWLEDs with diffused nanorod reflector and with ZnO nanorod antireflection layer. The FCWLEDs with diffused nanorod reflector and 250-nm-long ZnO nanorod antireflection layer was named FCWLED A, hereafter. The FCWLEDs with diffused nanorod reflector and without 250-nm-long ZnO nanorod antireflection layer (named FCWLED B, hereafter) were also fabricated for comparison.

3. Result and Discussion

To find the optimal rod-length of the ZnO nanorod in the antireflection layer, the performances of the GaN-based FCLEDs with diffused nanorod reflector and with 0-, 100-, 250-, 500-, and 750-nm-long ZnO nanorod arrays were firstly investigated. Figure 2 shows the light output power-current (L-I) curves of the GaN-based FCLEDs with diffused nanorod reflector and with ZnO nanorod arrays of various rod-lengths measured using an integrating sphere. As shown in Figure 2, the light output power of

the FCLEDs with diffused nanorod reflector and with 250-nm-long ZnO nanorod array was improved from 30.85 mW to 34.99 mW, compared with the FCLEDs with diffused nanorod reflector and without ZnO nanorod (i.e., 0-nm-long ZnO nanorod) antireflection layer at an injection current of 280 mA. However, when the rod-length of the ZnO nanorod array was longer than 250 nm, the light output power decreased owing to the absorption of the ZnO nanorod array. To confirm the optimal rod-length of the ZnO nanorod antireflection layer on the output side of the FCLEDs with diffused nanorod reflector, the standard optical software TracePro was also used to simulate the light propagated within the ZnO nanorod arrays of various rod-lengths. Figure 3 shows the simulating results of an enhancement in the illumination efficiency for the FCLEDs with diffused nanorod reflector and with ZnO nanorod antireflection layer of various rod-lengths, in comparison with the FCLEDs with diffused ZnO nanorod reflector and without ZnO nanorod antireflection layer. The illumination efficiency of the FCLEDs with diffused nanorod reflector and with 100-, 250-, 500-, and 750-nm-long ZnO nanorod antireflection layer shown an increase of 10.47%, 11.97%, 9.32%, and 8.33%, respectively. The experimental results of the enhanced proportion of the light output power for the resulted FCLEDs are also shown in Figure 3. The experimental results and the simulation results had the similar tendency. In addition, the optimal effective refractive index of the antireflection layer can be

determined by the formula of $(n_{air} \times n_{GaN})^{1/2}$, where n_{air} of 1.00 and n_{GaN} of 2.40 were the refractive index of air and n-GaN, respectively. The solution of the optimal effective refractive index of the antireflection layer was 1.55. In this work, the effective refractive index of the 250-nm-long ZnO nanrod antireflection layer was measured by an ellipseometer and the value was about 1.57 which was similar to the optimal effective refractive index of the antireflection layer. Therefore, the rod-length of 250 nm in the ZnO nanorod antireflection layer was the optimal length for the FCLEDs.

Figure 4 shows the electroluminescence (EL) spectra of the FCWLEDs with diffused nanorod reflector and with and without 250-nm-long ZnO nanorod antireflection layer (FCWLED A and FCWLED B) at an injection current of 20 mA. The EL spectra of the blue FCLEDs with diffused nanorod reflector and with 250-nm-long ZnO nanorod antireflection layer (named FCLED C, hereafter) and the blue FCLEDs with diffused nanorod reflector and without 250-nm-long ZnO nanorod antireflection layer (named FCLED D, hereafter) are also shown in Figure 4. As shown in Figure 4, the light-emission intensity of FCWLED A was larger than that of FCWLED B at the wavelength range from 400 nm to 700 nm. The light-emission intensity of FCLED C and FCLED D had the same situation. The improvement of the light-emission intensity was attributed to that the 250-nm-long ZnO nanorod

antireflection layer could effectively reduce the total reflection loss. The phosphor conversion efficiency η of the FCWLEDs was defined as:

$$\eta = \frac{P_{phosphor}}{P_p - P_{phosphor}} \quad (1)$$

where P_p is the optical power emitted from the blue FCLEDs without phosphor layer and $P_{phosphor}$ is the optical power converted from the phosphor layer. Compared with the FCWLED B, the phosphor conversion efficiency of FCWLED A operated at an injection current of 20 mA was improved from 77.6% to 80.1%. The improvement was attributed to that the ZnO nanorod antireflection layer could reduce the light total reflection at the sapphire surface, which could guide more blue light to pump the phosphor layer. Generally, the phosphor conversion efficiency as a function of the injection current of the LEDs. Consequently, the EL spectra of the FCLED C and FCWLED A at various injection currents were measured and are shown in Figure 5 (a) and (b), respectively. Using the experimental results and Eq. (1) to estimate the phosphor conversion efficiency of FCWLED A at various injection currents were measured and is shown in Figure 6. The phosphor conversion efficiency of FCWLED A was enhanced with an increased of the injection current, a maximum value of 92.5% was obtained as the FCWLED A operated at a current of 80 mA. This phenomenon was attributed to that the phosphor conversion efficiency reached saturation at an injection current of 80 mA. Therefore, when the injection current was

more than 80 mA, the phosphor conversion efficiency decreased owing to the excess blue light directly emitted out the FCWLEDs or the excess photons multi-scattered with the phosphor and were absorbed inside the FCWLEDs. The L-I curves of FCWLED A and FWCLED B were also measured using an integrating sphere system. The light output power of FCWLED A and FWCLED B was 23.90 mW and 21.15 mW, respectively, at an injection current of 280 mA.

Figure 7 shows the chromaticity diagram of FCWLED A and FCWLED B at an injection current of 80 mA. As shown in Figure 7, the chromaticity coordinate of the emission of the corresponding LEDs exhibited the same coordinate of (0.335, 0.333), which demonstrated that the emitted light was a white light.

4. Conclusions

The light output power and phosphor conversion efficiency of the FCWLEDs were successfully improved by using the diffused nanorod reflector and the ZnO nanorod antireflection layer. The diffused nanorod reflector constructed by the 500-nm-long ZnO nanorod arrays and the high reflective Al metal could effectively enhance the probability of light reflectivity from the bottom of the FCWLEDs. Moreover, according to the experimental results and the simulation results, the optimal 250-nm-long ZnO nanorods grown on the output side of the LEDs as the

antireflection layer could guide more blue light and could excite more phosphor to enhance the phosphor conversion efficiency. The light output power of the FCWLEDs with diffused nanorod reflector and with ZnO nanorod antireflection layer was enhanced 13.0% in comparison of the FCWLEDs with diffused nanorod reflector and without with ZnO nanorod antireflection layer at injection current of 280 mA. The phosphor conversion efficiency was also improved 2.5%.

Acknowledgement

This work was supported by the Industrial Technology Research Institute, Bureau of Energy, Ministry of Economic Affairs of Taiwan, Contract No. 102-E0605, the National Sciences Council of Taiwan under Grant NSC-101-2923-E-006-004-MY2, and the Advanced Optoelectronic Technology Center, National Cheng Kung University, Taiwan.

References

[1] H. Rao, W. Wang, X. L. Wan, L. S. Zhou, J.Y. Liao, D. Zhou, Q. L. Lei, and X. M. Wang, "An improved slurry method of self-adaptive phosphor coating for white pc-LED packaging," *J. Disp. Technol.*, vol. 9, no. 6, pp. 453–458, 2013.

[2] C. T. Lee and T. J. Wu, "Light distribution and light extraction improvement mechanisms of remote GaN-based white light-emitting-diodes using ZnO nanorod array," *J. Lumin.*, vol. 137, no. 5, pp. 143–147, 2013.

[3] Z. Y. Mao, Y. C. Zhu, L. Gan, Y. Zeng, F. F. Xu, Y. Wang, H. Tian, L. Li, and D. J. Wang, "Tricolor emission $Ca_3Si_2O_7$:Ln (Ln=Ce, Tb, Eu) phosphors for near-UV white light-emitting-diode," *J. Lumin.*, vol. 134, no. 2, pp. 148–153, 2013.

[4] S. H. Park, K. H. Lee, S. Unithrattil, H. S. Yoon, H. G. Jang, and W. B. Im, "Melilite-structure $CaYAl_3O_7:Eu^{3+}$ phosphor: structural and optical characteristics for near-UV LED based white light," *J. Phys. Chem.*, vol. 116, no. 51, pp. 26850–26856, 2012.

[5] S. Muthu, F. J. P. Schuurmans, and M. D. Pashley, "Red, green, and blue LEDs for white light illumination," *IEEE J. Sel. Top. Quantum Electron.*, vol. 21, no. 2, pp. 333–338, 2002.

[6] D. S. Kuo, S. J. Chang, T. K. Ko, C. F. Shen, S. J. Hon, and S. C. Hung, "Nitride-based LEDs with phosphoric acid etched undercut sidewalls," *IEEE Photon. Technol. Lett.*, vol. 21, no. 8, pp. 510–512, 2009.

[7] S. E. Brinkley, C. L. Keraly, J. Sonoda, C. Weisbuch, J. S. Speck, S. Nakamura, and S. P. DenBaars, "Chip shaping for light extraction enhancement of bulk c-plane light-emitting diodes," *Appl. Phys. Express*, vol. 5, no. 3, pp. 032104-1–032104-3, 2012.

[8] H. Y. Lee, X. Y. Huang, and C. T. Lee, "Light output enhancement of GaN-based roughened LEDs using bias-assisted photoelectrochemical etching method," *J. Electrochem. Soc.*, vol. 155, no. 10, pp. H707–H709, 2008.

[9] C. C. Lin and C. T. Lee, "Enhanced light extraction of GaN-based light emitting diodes using nanorod arrays," *Electrochem. Solid State Lett.*, vol. 13, no. 8, pp. H278–H280, 2010.

[10] D. H. Kim, C. O. Cho, Y. G. Roh, H. Jeon, Y. S. Park, J. Cho, J. S. Im, C. Sone, Y. Park, W. J. Choi, and Q. H. Park, "Enhanced light extraction from GaN-based light-emitting diodes with holographically generated two-dimensional photonic crystal patterns," *Appl. Phys. Lett.*, vol. 87, no. 20, pp. 203508-1–203508-3, 2005.

[11] H. K. Cho, J. Jang, J. H. Choi, J. Choi, J. Kim, J. S. Lee, B. Lee, Y. H. Choe, K.

D. Lee, S. H. Kim, K. Lee, S. K. Kim, and Y. H. Lee, “Light extraction enhancement from nano-imprinted photonic crystal GaN-based blue light-emitting diodes,” *Opt. Express*, vol. 14, no. 19, pp. 8654–8660, 2006.

[12] Y. C. Chang, J. K. Liou, and W. C. Liu, “Improved light extraction efficiency of a high-power GaN-Based light-emitting diode with a three-dimensional-photonic crystal (3-D-PhC) backside reflector,” *IEEE Electron Device Lett.*, vol. 34, no. 6, pp. 777-779, 2013.

[13] N. Lobo, H. Rodriguez, A. Knauer, M. Hoppe, and S. Einfeldt, “Enhancement of light extraction in ultraviolet light-emitting diodes using nanopixel contact design with Al reflector,” *Appl. Phys. Lett.*, vol. 96, no. 8, pp. 081109-1–081109-3, 2010.

[14] X. Yan, M. Shatalov, T. Saxena, and M. S. Shur, “Deep-ultraviolet tailored- and low-refractive index antireflection coatings for light-extraction enhancement of light-emitting diodes,” *J. Appl. Phys.*, vol. 113, no. 16, pp. 163105-1–163105-5, 2013.

[15] C. T. Lee and C. Y Chuang, “Light extraction enhancement of GaN-based flip-chip light-emitting diodes using diffused nanorod reflector,” *Appl. Phys. Express*, vol. 5, no. 11, pp. 112104-1–112104-3, 2012.

[16] C. T. Lee and H. W. Kao, “Long term thermal stability of Ti/Al/Pt/Au ohmic

contacts to n-type GaN," *Appl. Phys. Lett.*, vol. 76, no. 17, pp. 2364–2366, 2000.

[17] C. S. Lee, Y. J. Lin, and C. T. Lee, "Investigation of oxidation mechanism for ohmic formation in Ni/Au contacts to p-type GaN layers," *Appl. Phys. Lett.*, vol. 79, no. 23, pp. 3815–3817, 2001.

Figure captions

FIGURE 1 The schematic configuration of the GaN-based FCWLEDs with diffused nanorod reflector and with ZnO nanorod antireflection layer. The inset figure shows the morphology of diffused nanorod reflector.

FIGURE 2 The light output power-current curves of the GaN-based FCLEDs with diffused nanorod reflector and with ZnO nanorod antireflection layers of various rod-lengths.

FIGURE 3 The simulating results and experimental results of the enhancement in the illumination efficiency and light output power for the resulted FCLEDs and FCWLEDs with ZnO nanorod antireflection layers of various rod-lengths, in comparison with the resulted FCLEDs and FCWLEDs without ZnO nanorod antireflection layer, respectively.

FIGURE 4 The electroluminescence spectra of the resulted FCWLEDs and FCLEDs with and without 250-nm-long ZnO nanorod antireflection layer at an injection current of 20 mA.

FIGURE 5 The electroluminescence spectra of (a) FCLED C and (b) FCWLED A at various injection currents.

FIFURE 6 The phosphor conversion efficiency of FCWLED A at various injection currents.

FIGURE 7 The chromaticity diagram of FCWLED A and FCWLED B.

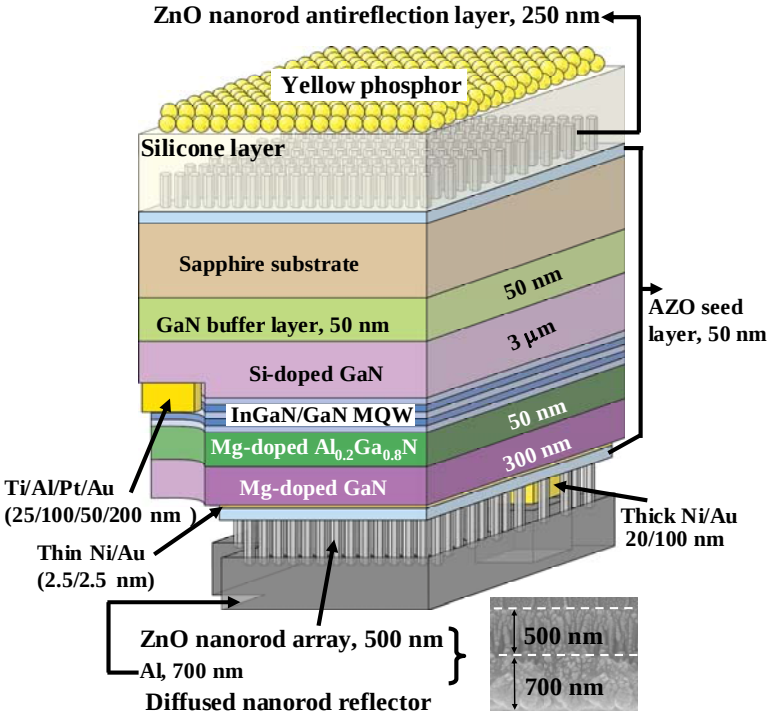
ZnO nanorod antireflection layer, 250 nm
Yellow phosphor
Silicone layer
Sapphire substrate
GaN buffer layer, 50 nm
Si-doped GaN
InGaN/GaN MQW
Mg-doped Al0.2Ga0.8N
Mg-doped GaN
50 nm
3 μm
50 nm
300 nm
AZO seed layer, 50 nm
Ti/Al/Pt/Au (25/100/50/200 nm)
Thin Ni/Au (2.5/2.5 nm)
Thick Ni/Au 20/100 nm
ZnO nanorod array, 500 nm
Al, 700 nm
Diffused nanorod reflector
500 nm
700 nm

FIGURE 1

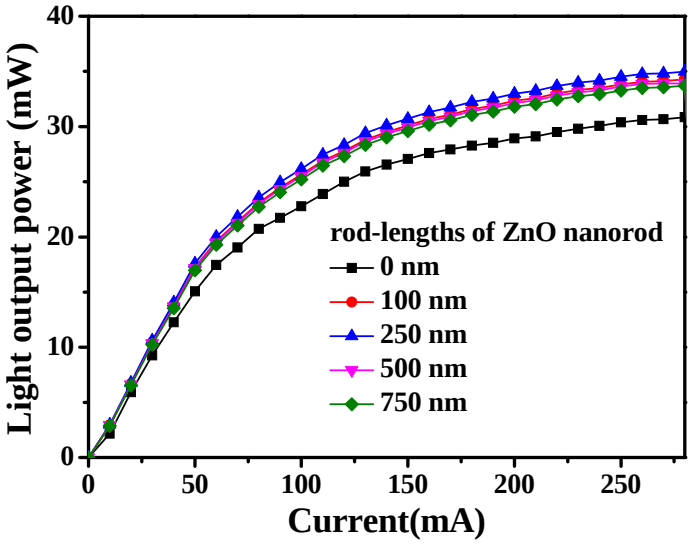
Light output power (mW)
Current(mA)
0
10
20
30
40
0
50
100
150
200
250
rod-lengths of ZnO nanorod
0 nm
100 nm
250 nm
500 nm
750 nm

FIGURE 2

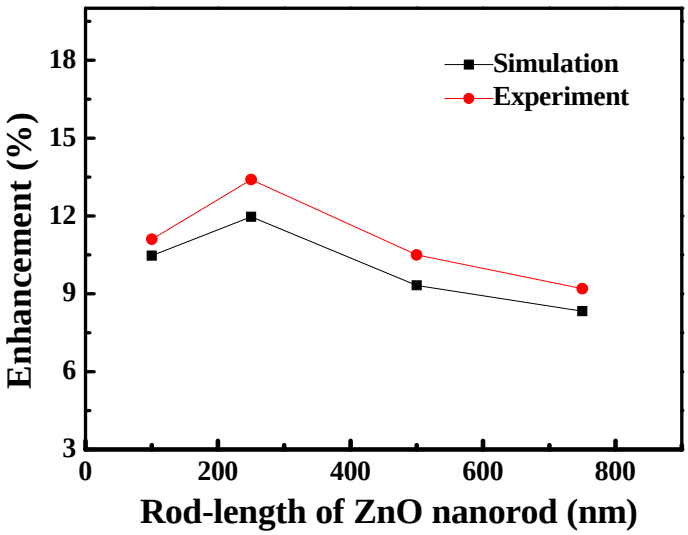
Simulation
Experiment
Enhancement (%)
18
15
12
9
6
3
0
200
400
600
800
Rod-length of ZnO nanorod (nm)

FIGURE 3

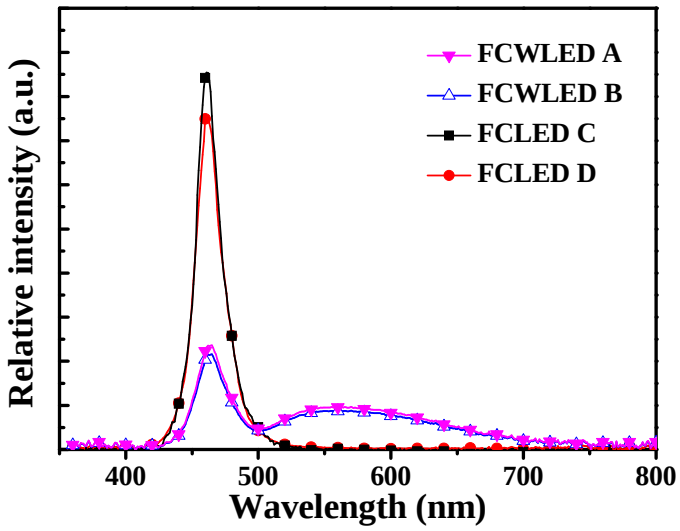
Relative intensity (a.u.)
Wavelength (nm)
400
500
600
700
800
FCWLED A
FCWLED B
FCLED C
FCLED D

FIGURE 4

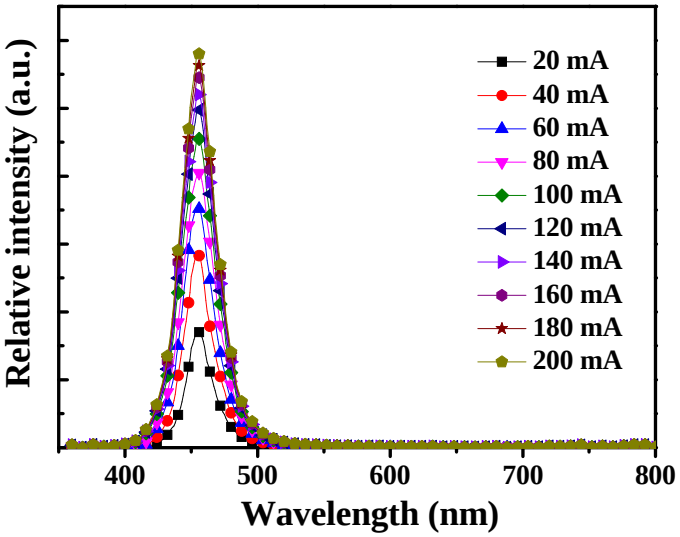
Relative intensity (a.u.)
Wavelength (nm)
400
500
600
700
800
20 mA
40 mA
60 mA
80 mA
100 mA
120 mA
140 mA
160 mA
180 mA
200 mA

(a)

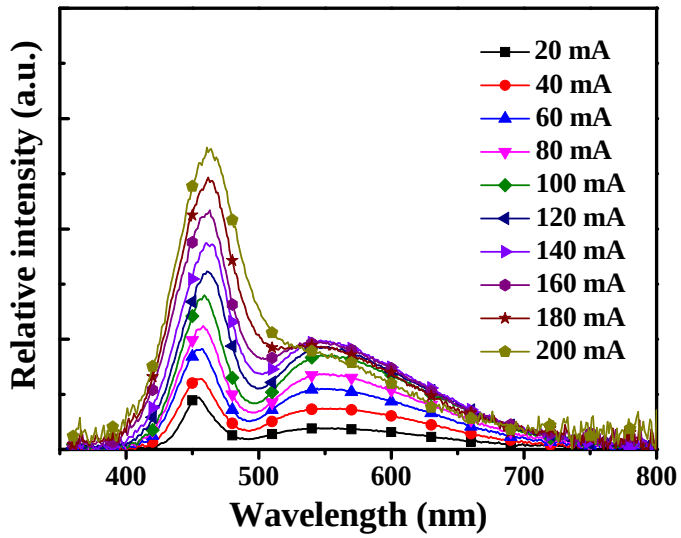
Relative intensity (a.u.)
Wavelength (nm)
400
500
600
700
800
20 mA
40 mA
60 mA
80 mA
100 mA
120 mA
140 mA
160 mA
180 mA
200 mA

(b)

FIGURE 5

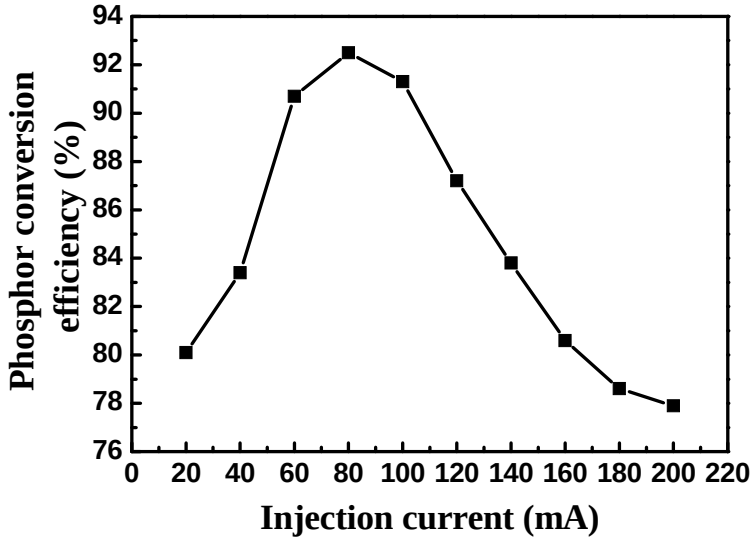
Phosphor conversion efficiency (%)
94
92
90
88
86
84
82
80
78
76
0
20
40
60
80
100
120
140
160
180
200
220
Injection current (mA)

FIGURE 6

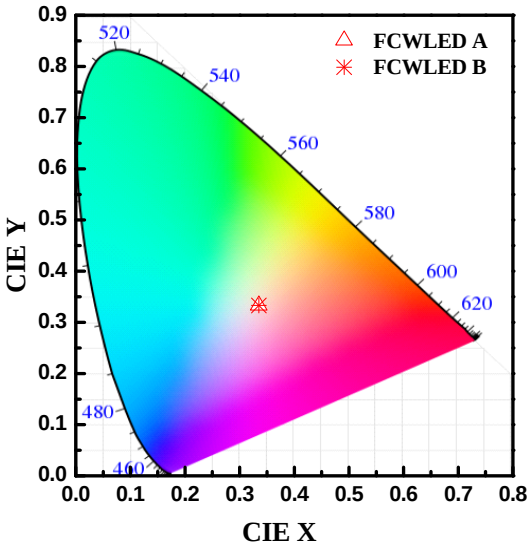
FCWLED A
FCWLED B
520
540
560
580
600
620
480
460
CIE Y
CIE X
0.0
0.1
0.2
0.3
0.4
0.5
0.6
0.7
0.8
0.9

FIGURE 7